MEASUREMENT OF THE GALACTIC X-RAY/ γ -RAY BACKGROUND RADIATION: CONTRIBUTION OF DISCRETE SOURCES

Azita Valinia^{1,2}, Robert L. Kinzer³, and Francis E. Marshall¹

Accepted for Publication in the Astrophysical Journal

ABSTRACT

The Galactic background radiation near the Scutum Arm was observed simultaneously with RXTE and OSSE in order to determine the spectral shape and the origin of the emission in the hard X-ray/soft γ -ray band. The spectrum in the 3 keV to 1 MeV band is well modeled by 4 components: a high energy continuum dominating above 500 keV that can be characterized by a power law of photon index ~ 1.6 (an extrapolation from measurements above $\sim 1 \text{ MeV}$); a positron annihilation line at 511 keV and positronium continuum; a variable hard X-ray/soft γ -ray component that dominates between 10-200 keV (with a minimum detected flux of $\sim 7.7 \times 10^{-7}$ photons cm⁻² s⁻¹ keV⁻¹ deg⁻² at 100 keV averaged over the field of view of OSSE) and that is well modeled by an exponentially cut off power law of photon index ~ 0.6 and energy cut off at ~ 41 keV; and finally a thermal plasma model of solar abundances and temperature $\sim 2.6 \text{ keV}$ that dominates below 10 keV. We estimate that the contribution of bright discrete sources to the minimum flux detected by OSSE was $\sim 46\%$ at 60 keV and $\sim 20\%$ at 100 keV. The remaining unresolved emission may be interpreted either as truly diffuse emission with a hard spectrum (such as that from inverse Compton scattering) or the superposition of discrete sources that have very hard spectra.

Subject headings: galaxies: individual (Milky Way) — ISM: structure — X-rays: ISM — gamma rays: observations — cosmic rays

¹Laboratory for High Energy Astrophysics, Code 662, NASA/Goddard Space Flight Center, Greenbelt, MD 20771; valinia@milkyway.gsfc.nasa.gov

²Department of Astronomy, University of Maryland, College Park, MD 20742

³E. O. Hulburt Center for Space Research, Naval Research Laboratory, Washington, DC 20375-5352

1. INTRODUCTION

Since its discovery, the Galactic X-ray/ γ -ray background, particularly from the ridge (i.e. the narrow region centered on the plane covering approximately $\pm 60^{\circ}$ in longitude), has been studied with every major X-ray and γ -ray observatory. The spectrum of the emission is reasonably well measured and understood above ~ 1 MeV (e.g., Kinzer, Purcell, & Kurfess 1999; Strong et al. 1996a; Bloemen et al. 1997; Hunter et al. 1997; Hunter, Kinzer, & Strong 1997). At energies above 100 MeV, the dominant emission process is the decay of π^0 meson produced in the interaction of cosmic ray nucleons with the interstellar matter (e.g., Bertsch et al. 1993). Between ~ 1 and 70 MeV, electron bremsstrahlung and inverse Compton scattering appear to dominate over discrete sources (e.g., Sacher & Schönfelder 1984; Kniffen & Fitchel 1981, Skibo 1993). However, in the hard X-ray/soft γ -ray band (3-500 keV) the shape of the spectrum and the origin of the emission remain uncertain. At soft γ -ray energies (below 1 MeV), multiple components are believed to contribute to the total emission. These include transient discrete sources, positron annihilation line and 3-photon positronium continuum radiation, and a soft γ -ray component dominant up to about 300 keV of unknown origin. This component, measured with the CGRO's Oriented Scintillation Spectrometer Experiment (OSSE), can be roughly characterized by simple power law models of indices between 2.3 and 3.1 at different locations on the Galactic plane (e.g., Kinzer et al. 1999; Skibo et al. 1997). More recently, the soft γ -ray emission from the Galactic center was measured by the HIREGS balloon-borne germanium spectrometer and was characterized by a single power law of photon index ~ 1.8 plus the positronium component (Boggs et al. 1999). However, many of the soft γ -ray observations, particularly those from the central region of the Galaxy, are contaminated by bright and variable discrete sources. At hard X-ray energies (10-35 keV), the overall spectrum of the Galactic plane background was characterized by a power law of photon index ~ 1.8 with RXTE (Valinia & Marshall 1998; hereafter VM98). Hard X-ray emission above 10 keV was also detected with Ginga (Yamasaki et al. 1997).

How the spectral shape of the background radiation extends from the hard X-ray to the soft γ -ray regime and how much of the emission is due to discrete sources remains to be determined and is the subject of this paper. Determining the exact nature of the spectrum in this band has significant implications for the energetics of the Interstellar Medium (ISM). For example, a power law spectrum extending from 10 keV to 1 MeV, if interpreted to be of diffuse nonthermal origin, has been proposed to result from nonthermal electron bremsstrahlung (e.g. Skibo et al. 1997). However this process is energetically very demanding since electron bremsstrahlung at these energies is highly inefficient. A power of $10^{42} - 10^{43} \,\mathrm{erg \, s^{-1}}$ is required, which approaches or even exceeds the power injected into the Galaxy via supernovae explosions (Skibo et al. 1997). Attempting to explain the nature of the emission in terms of diffuse thermal processes is equally unsatisfactory because plasma

temperatures of 80-100 keV are implied. Since the gravitational potential of the Galaxy is only on the order of 0.5 keV, it is not clear how such a plasma would be generated and confined to the Galactic plane.

Unfortunately, measurement of the Galactic background radiation in the hard X-ray/soft γ -ray band and its interpretation is inherently difficult with current instruments because of the presence of numerous transient, hard discrete sources in the Galactic plane, and the fact that generally hard X-ray/ γ -ray instruments either have large fields of view and no imaging capabilities or have imaging capability but no diffuse emission sensitivity. As a result, distinction of diffuse emission from point sources with current instruments has remained a difficult task. For this reason, simultaneous, multiple instrument observations are necessary. To date, coordinated observations of the Galactic center region with OSSE and the imaging instrument SIGMA has been performed (Purcell et al. 1996). However, SIGMA has a sensitivity of about 25 mcrab (2σ) for a typical 24 hour observation. As a result, weak sources escape detection in such a survey and the unresolved spectrum can still be significantly contaminated by discrete source contribution.

In this paper, we present contemporaneous observations of the Galactic background emission near the Scutum Arm (centered at $l=33^{\circ}$) over the 3 keV to 1 MeV range with RXTE and OSSE. RXTE has a relatively small field of view of 1° FWHM with hard X-ray capability and discrete source sensitivity of ~ 1 mcrab in the 2-10 keV band, making the detection of hard, discrete sources in the field of view of OSSE possible. OSSE, with a field of view of 11°.4 × 3°.8 FWHM, is sensitive to diffuse emission in the soft γ -ray band. The Scutum Arm was chosen because it exhibits bright and apparently diffuse emission (e.g. Kaneda 1997; VM98), and unlike the Galactic center region for example, there are few bright discrete sources in the field of view. This direction is approximately tangent to the 5-kpc arm of our Galaxy as seen from the Earth. The arm contains large numbers of young stars (Hayakawa et al. 1981), and an unusual concentration of high-mass X-ray binary transients (van Paradijs 1995). Our main goal is to constrain the shape of the spectrum and understand its origin in the 10 – 400 keV band. In §2 we present our observations and in §3 we present the results of our analysis. Finally in §4 we discuss their implications.

2. OBSERVATIONS

The simultaneous RXTE and OSSE observations were performed from January 28 through February 23 of 1998. The OSSE instrument (Johnson et al. 1993) consists of four Na(TI)/CsI(Na) phoswich detectors which cover the energy range 50 keV-10 MeV. It has an effective area of $\sim 2000 \, \mathrm{cm}^2$ and average energy resolution of $\sim 8.8\%$ at 511 keV. The

field of view is approximately rectangular with FWHM of $11^{\circ}.4 \times 3^{\circ}.8$. During the 4 weeks of observation, OSSE (with its long collimator axis parallel to the Galactic plane) was continuously oriented toward Galactic coordinates $(l,b)=(33^{\circ},0^{\circ})$ except for alternating 2-minute intervals during which offset background measurements were made. The background was taken alternately at Galactic latitudes $\pm 9^{\circ}$ ($l=33^{\circ}$) during weeks 1 and 3 of the observation and $\pm 12^{\circ}$ ($l=33^{\circ}$) during weeks 2 and 4 of the observation.

The RXTE observations were planned such that during the 4 week observation, RXTE was scanning the full field of view of OSSE (i.e. the region $44^{\circ} < l < 22^{\circ}$ and $-4^{\circ} < b < 4^{\circ}$) every day for either one or two hours (exposures alternated between one and two hour intervals). The goal of these observations were two-fold. One was to monitor discrete sources in the field of view of OSSE and to estimate their contribution to OSSE's flux. The second goal was to measure the spectrum of the diffuse emission in the hard X-ray band and simultaneously model that with the spectrum measured with OSSE. The RXTE scans were performed with the Proportional Counter Array (PCA). The PCA (Jahoda et al. 1996) has a total collecting area of 6500 cm², an energy range of 2-60 keV, and energy resolution of $\sim 18\%$ at 6 keV. The field of view of the collimator is approximately circular with FWHM of 1°. The RXTE "diffuse" emission spectrum was obtained by scanning the field of view of OSSE excluding the regions that the scans went over known and detected discrete sources. The most recent PCA background estimator program pcabackest (version 2.0c; L7 model) provided by the RXTE Guest Observer Facility was used to estimate the PCA background.

3. ANALYSIS

Figure 1 shows the composite diffuse plus discrete-source emission spectrum as measured by OSSE in weeks 1 and 2 (filled circles - hereafter W1-2) and weeks 3 and 4 (open circles-hereafter W3-4) of the observations. The lowest energy data point for each observation has an approximately 20% systematic uncertainty and was therefore not used for modeling the data. In order to convert the flux through the OSSE collimator to the diffuse flux per radian of the Galaxy, a 5° FWHM Gaussian distribution in latitude and constant intensity in longitude for the spatial distribution of the emission was assumed (e.g., Kinzer et al. 1999; Purcell et al. 1996). In the 8-35 keV band, the FWHM of the distribution was derived to be $4^{\circ}.8^{+2.4}_{-1.0}$ with RXTE (VM98). The converted flux per radian is therefore a function of this latitude assumption. For example, assuming a FWHM of 2° would lower the flux per radian by $\sim 30\%$. Assuming a FWHM of 8° would increase the flux per radian by $\sim 50\%$ (see Figure 4 of Kinzer et al. 1999). We will discuss how this assumption affect the spectral fits in §3.2.

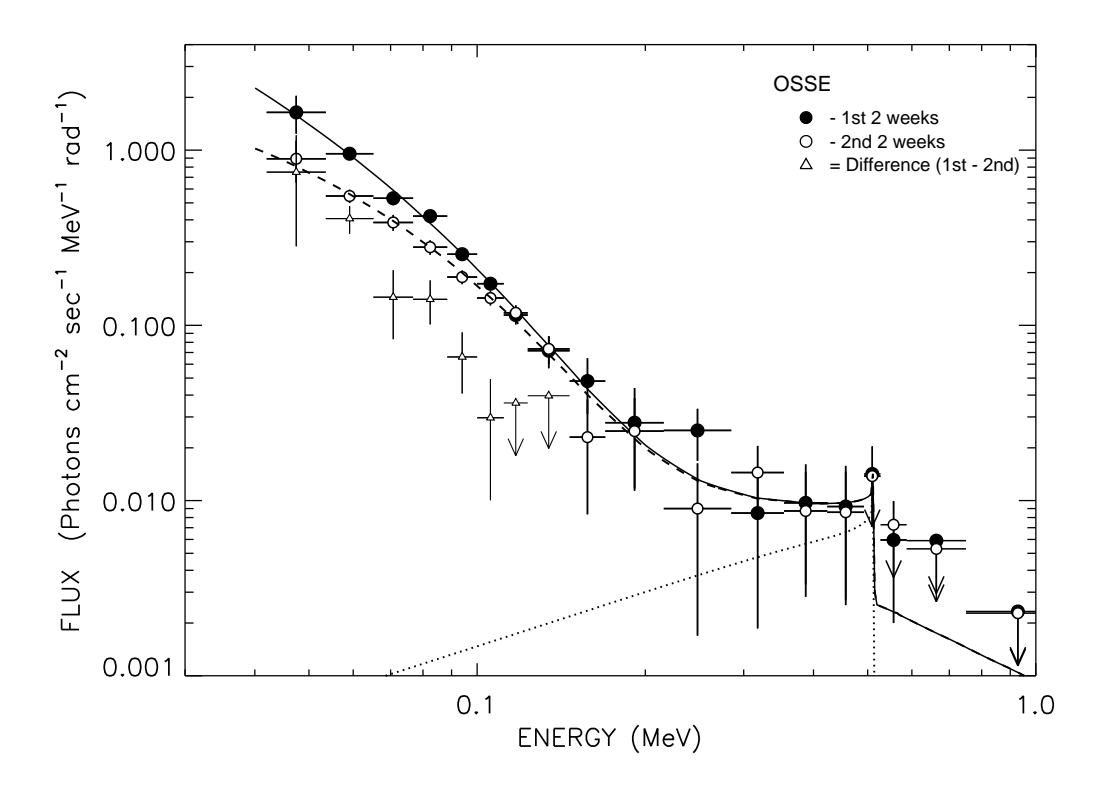


Fig. 1.— Emission spectrum as measured by OSSE in weeks 1 and 2 (filled circles) and weeks 3 and 4 (open circles). Diffuse emission of Gaussian distribution with FWHM of 5° in latitude and constant in longitude has been assumed for OSSE's response. The spectrum can be modeled by a composite of 3 components: a soft γ -ray component; positron annihilation line (at 511 keV) and 3-photon positronium continuum; and extrapolation of the high energy continuum from above 0.5 MeV. The solid and dashed line indicate the overall composite best fit models in the first half and second half of observations, respectively. The dotted line indicates the positron annihilation component from the full 4-week observation. Note that the lowest energy point for each observation has an approximately 20% systematic uncertainty and was not used in modeling the data.

As seen from Figure 1, the spectra in the 40 keV to 1 MeV range from the two viewing periods are similar except in the $\sim 40-100$ keV energy range where variable discrete sources have apparently altered the shape of the spectrum. The intensity in the 60-100 keV band dropped by about 32% between the two viewing periods. The difference spectrum of the two viewing periods (triangles in Figure 1) can be modeled by a power law of photon index ~ 4.3 . In what follows, we first discuss the detection and estimated contribution of discrete sources to the total OSSE flux. We then discuss the modeling and characteristics of the measured RXTE/OSSE spectra.

3.1. Discrete Sources

Table 1 lists bright X-ray sources detected during the PCA scans that were within the field of view of OSSE. It also includes GRS 1915+105, which is near the edge of the field of view, since it is known to be extremely variable with intensities as high as a few Crabs (e.g., Muno et al. 1999). The first four sources are accretion-driven pulsars while the last two sources are microquasars. The spectra of these sources could not be well determined above 20 keV with our RXTE observations because the scans had insufficient exposure time. For each of these sources, we determined a spectral shape from other reported observations and estimated their 60 and 100 keV flux by normalizing their spectra with the average 2-10 keV flux during the PCA scans. We used public RXTE data for XTE J1858+034 (from observations on Feb. 20 and 24, 1998) and GS 1843+009 (from March 5, 1997). For both of these sources we model the photon distribution using the standard form for pulsars

$$A(E) = k(E/1 \text{ keV})^{-\Gamma} \exp((E_c - E)/E_f)$$
(1)

(e.g. White, Swank, & Holt 1983). For XTE J1858+034, we find $\Gamma \sim 1.3$, $E_c \sim 2.3$ and $E_f \sim 24.6$. For GS 1843+009, we find $\Gamma \sim 0.6$, $E_c \sim 13.3$ and $E_f \sim 22.3$. Koyama et al. (1990) found similar parameters ($\Gamma \sim 0.71$, $E_c \sim 18.3$ and $E_f \sim 25$) during the 1988 observations with Ginga when the source intensity varied between 30 and 60 mCrabs. In the case of A1845-024 (also identified as GRO 1849-03), we used the BATSE spectrum of this source during outburst reported by Zhang et al. (1996) characterized by a power law of $\Gamma \sim 2.8$. For XTE J1855-026, we used the RXTE spectrum reported by Corbet et al. (1998) characterized by the pulsar model (equation 1) and parameters $\Gamma \sim 1.23$, $E_c \sim 14.7$ and $E_f \sim 27$. For SS433, we used an exponentially cutoff power law model of photon index 1.5 and cutoff energy at 20 keV (Band, private communication, 1999). During our observations, GRS1915+105 was in a very soft spectral state with an average power law photon index of ~ 5.7 and was not detected with RXTE above 40 keV (Muno & Morgan 1999, private communication; Heindl 1999, private communication).

According to our estimate, the integrated 60-100 keV flux of the combined known bright sources listed in Table 1 (as would be seen through the OSSE's collimator) decreased by about 41% (from $(1.22 \pm 0.12) \times 10^{-3}$ to $(7.14 \pm 0.66) \times 10^{-4}$ photons cm⁻² s⁻¹) from the first viewing period (W1-2) to the second viewing period (W3-4) while the total OSSE measured flux for the entire field of view dropped by 32% (from $(3.68 \pm 0.15) \times 10^{-3}$ to $(2.50 \pm 0.11) \times 10^{-3}$ photons cm⁻² s⁻¹). It appears that the unresolved portion of the emission (i.e. total OSSE flux minus the estimated contribution of discrete sources flux) has also decreased from the first to the second viewing period. We offer two plausible explanation for this. One is that if indeed, the residual flux is made of discrete sources, this implies that the intensity of the integrated unresolved sources as seen through the OSSE collimator has also

decreased. There may be a tendency to believe that the integrated contribution of hundreds of discrete sources cannot change very much. However, the integrated contribution can easily be dominated by one or two sources. If these sources are highly variable as shown in Table 1, then the integrated flux can also vary substantially. Furthermore, RXTE's total monitoring time amounts to only $\sim 7\%$ of the total observation time by OSSE. If these sources showed substantial variability on the order of a day, it is possible that a potential source outburst escaped detection by RXTE but its flux was continuously measured with OSSE. Another explanation is that the apparent decrease in the unresolved flux is due to inaccuracies in our estimates of the contribution of known sources to the emission. These estimates are unavoidably uncertain because they use spectral fits from other observations and the spectral fits are generally at energies below 50 keV. Consequently spectral variations with time or deviations from the assumed spectral model will lead to errors in the estimated fluxes. In particular, since the 2-10 keV fluxes are generally lower during the second viewing interval, luminosity dependent spectral changes will cause systematic differences in the estimated fluxes for the two observing intervals. For example, from Table 1 it appears that GS 1843+009 is the dominant contributor among discrete sources. During the first viewing period, the 2-10 keV flux of this source was a factor of 2.7 lower than that measured during its bright state observed on March 5, 1997, and the flux was a factor of ~ 5 lower during the second viewing period. We have assumed the same spectral shape for both observations. We are not aware of a comprehensive study documenting the relation between luminosity and spectral shape of pulsars, but there is some evidence that the spectrum of accretion-driven pulsars depends on luminosity. Reynolds, Parmar, & White (1993) found that the spectrum at low energies became harder and E_c decreased as the luminosity of the transient pulsar EXO 2030+375 decreased during an outburst. As a result, the ratio of the extrapolated hard X-ray (50-100 keV) flux to the 2-10 keV flux decreased as the source luminosity decreased. The hardness ratio "HR", defined as the ratio of the flux at 50 keV to the flux at 5 keV, decreased by ~ 2 as the luminosity decreased by ~ 25 from $1.0 \times 10^{38}\,\mathrm{ergs\,s^{-1}}$. On the other hand, Koyama et al. (1990) did not find luminosity dependent spectral changes for GS 1843+009 while the source varied by a factor of ~ 2 . If the spectrum of GS 1843+009 during the OSSE measurements is softer than the spectrum measured when it was more luminous, then its contributions to the OSSE measurements have been overestimated, particularly in the second viewing period when the source luminosity was a factor of 5 lower than the bright state observation of March 5, 1997. A factor of 2 decrease in the contribution of GS 1843+009 would increase the residual flux at 60 keV from 5.8×10^{-5} to 7.2×10^{-5} photons cm⁻² s⁻¹ for the second observing interval. This decreases the difference in the residual fluxes for the two viewing intervals (the residual flux at 60 keV for the first viewing period was determined to be 10.1×10^{-5} photons cm⁻² s⁻¹ from Table 1). The fact that Koyama et al. (1990) did not find luminosity dependent spectral changes for GS 1843+009 makes this explanation less compelling. We also note that the HR for our spectral model for GS 1843+009 is ~ 3 times larger than that of the Koyama et al. model and is also larger than that of any of the pulsars in the review of White, Swank, and Holt (1983). This suggests that the values in Table 1 may, in fact, be overestimates of the contributions of GS 1843+009.

Because of these uncertainties, we do not subtract the contribution of these sources from the OSSE spectrum reported in the next section but instead, we model *only* the OSSE data during the *second* viewing period when the intensity of discrete sources was the least.

3.2. Spectral Characteristics

3.2.1. OSSE data: 50-400 keV

We now focus on the spectral characteristics of the soft γ -ray Galactic background emission. As discussed by Kinzer et al. (1999), the gamma ray continuum between 50 keV and 10 MeV can be described by a composite of 3 independent components: (1) a soft γ -ray component dominant up to about 300 keV of uncertain origin; (2) a hard γ -ray component (hereafter high energy continuum or HE) which is the extrapolation of the HE component above 1 MeV and is likely due to the interaction of cosmic rays with the ISM dominating above 500 keV (e.g. Skibo 1993); (3) positron annihilation line and 3-photon positronium continuum radiation (hereafter PA; Ore & Powell 1949) which are strongly enhanced toward the Galactic center. Fits to the OSSE data accumulated during the entire 4 week observation were used to determine the best fit parameters for the HE and PA components since they are not expected to be variable with time (see Figure 1). The positronium continuum and narrow 511 keV annihilation line integral fluxes were $(2.0\pm0.7)\times10^{-3}$ and $(0.1 \pm 0.3) \times 10^{-3}$ photons cm⁻² s⁻¹ rad⁻¹, respectively. The HE continuum intensity was determined from fits to these data combined with the collected Galactic plane observations following Kinzer et al. (1999). The HE component extrapolated to energies below 1 MeV can be characterized as a power law function of photon index 1.6 and normalization of $3.6 \times 10^{-2} \,\mathrm{photons}\,\mathrm{cm}^{-2}\,\mathrm{s}^{-1}\,\mathrm{MeV}^{-1}\,\mathrm{rad}^{-1}$ at 100 keV.

Modeling the OSSE data *alone* from 50-400 keV (obtained from the second viewing period), we find that the best fit is achieved with an exponential cut off power law model

$$A(E) = k(E/1 \text{ keV})^{-\Gamma} \exp(-E/E_c)$$
(2)

plus the HE continuum included as a fixed model component ($\chi^2/\nu = 3.95/9$). (We have subtracted the PA components from the OSSE data points according to the results obtained from the 4 week combined observations). The best fit parameters for the power law are:

 $\Gamma = -0.2^{+1.2}_{-2.5}$ and $E_c = 30.1^{+47.3}_{-5.4}$ and a total flux (including the HE continuum) of 7.8×10^{-7} photons cm⁻² s⁻¹ keV⁻¹ deg⁻² at 100 keV averaged over the field of view of OSSE. All the quoted errors are for 90% confidence limit. Removing the HE component produces a worse fit $(\chi^2/\nu = 5.0/10)$ and yields a higher photon index and cut off energy that are within the 90% confidence limits of the previous fit. Without the HE component, the 50 – 400 keV data can also be satisfactorily fit $(\chi^2/\nu = 9.4/10)$ with a single power law $(A(E) = k(E/1 \,\mathrm{keV})^{-\Gamma})$ of photon index $\Gamma = 2.6 \pm 0.2$.

3.2.2. RXTE/OSSE data: 3-400 keV

We proceed by modeling the RXTE/OSSE spectra simultaneously using the OSSE spectrum obtained in the second viewing period, but the PA component subtracted from OSSE data. For the simultaneous fit, the flux normalization for the two instruments must be handled consistently. For extended emission, the measured flux depends on the field of view of each instrument and the spatial distribution of the diffuse emission. Hence, an effective solid angle (i.e. the convolution of the distribution of the emission with the detector's response function) should be calculated for each instrument. In the case of OSSE (fov of $11^{\circ}.4 \times 3^{\circ}.8$ FWHM), convolving the soft γ -ray Galactic diffuse emission (assuming a Gaussian latitude distribution with 5° FWHM) and OSSE 's triangular response function yields an effective solid angle of $\sim 1.3 \times 10^{-2}$ sr. RXTE 's solid angle is $\sim 3 \times 10^{-4}$ sr. Hence, a composite data set was obtained by scaling down the OSSE data by a factor of 2.3×10^{-2} to account for the difference in the solid angle of the two instruments. In fitting the combined data, the intensity model parameters for the two instruments has been set equal to each other. In all the models presented hereafter, the diffuse HE continuum is included as a fixed model component present at all energies. It contributes approximately 13% to the total emission in the 3-100 keV band. Generally, inclusion of this component tends to slightly improve the fit.

Examining the 10-400 keV spectrum first, we find that the excess over the HE diffuse component is best described by an exponentially cut off power law model (equation 2) with the following parameters ($\chi^2/\nu=24.8/43$): photon index $\Gamma=0.63\pm0.25$, energy cutoff $E_c=41.4^{+13.0}_{-8.4}$ keV, and flux of 6.0×10^{-7} photons cm⁻² s⁻¹ keV⁻¹ deg⁻² at 100 keV. The total flux (including the HE continuum flux) at 100 keV is 7.7×10^{-7} photons cm⁻² s⁻¹ keV⁻¹ deg⁻². Notice that the best fit parameters are within the 90% confidence limits of those derived from fitting the OSSE data alone but that they are considerably more tightly constrained.

As we discussed earlier, the flux intensity measured with OSSE depends on the assumption of latitude distribution of the diffuse emission. So far, we have presented results

assuming a Gaussian distribution of 5° FWHM in latitude. To explore how the results depend on this assumption, we have simultaneously fitted the RXTE data with the OSSE data scaled up and down by 50%, respectively, to allow for a different FWHM Gaussian distribution. Scaling up the OSSE data by 50% is equivalent to assuming a \sim 8° FWHM Gaussian distribution while scaling it down by 50% is equivalent to \leq 0°.1 FWHM. Scaling the OSSE data up yields a lower photon index ($\Gamma = 0.41^{+0.19}_{-0.17}$; $E_c = 41.7^{+9.5}_{-6.3}$ keV) while scaling it down will have the opposite effect ($\Gamma = 1.23^{+0.33}_{-0.29}$; $E_c = 51.6^{+37.8}_{-14.5}$ keV). In both cases, the fit is worse and the fit parameters are marginally consistent with the 90% confidence limits of those parameters derived for a 5° FWHM Gaussian assumption.

Other models with high-energy cutoffs of different forms also provide good fits. For the standard, 5° FWHM Gaussian distribution, the standard pulsar model (equation 1) yields $\Gamma = 0.8^{+0.6}_{-0.4}$, $E_c = 21.5^{+51.7}_{-21.5}$ keV, and $E_f = 45.3^{+20.3}_{-9.7}$ ($\chi^2/\nu = 24.3/42$). The best-fit ($\chi^2/\nu = 25.5/42$) Comptonized disk model (Sunyaev & Titarchuk 1980) has an input soft photon (Wien) temperature of < 1 keV, a plasma electron temperature of 21 keV, and a plasma optical depth of 3. A broken power law model with photon indices of 1.4 and 3.3 and a break energy at 75.2 keV also provides a good fit ($\chi^2/\nu = 29.0/42$), but a simple power law model (best fit photon index of 1.7) does not ($\chi^2/\nu = 97.3/44$).

We extended the RXTE/OSSE spectral fit down to 3 keV by adding a Raymond-Smith thermal plasma component to the exponentially cutoff power law model (and the HE continuum fixed in the model as before) and including the effect of Galactic absorption. The broader-range fit shown in Figure 2 yields $\chi^2/\nu = 54.0/60$. The 3-10 keV spectrum is dominated (71%) by the thermal plasma component. The best model yields a hydrogen column density of $N_H = 3.1 \pm 1.5 \times 10^{22} \, \mathrm{cm}^{-2}$ (the interstellar value for the line of sight at the center of the OSSE field of view is $\sim 2 \times 10^{22} \, \mathrm{cm}^{-2}$; the values for the lines of sight to the FWHM corners of the field of view are as low as $0.4 \times 10^{22} \, \mathrm{cm}^{-2}$), and a thermal plasma component of solar abundances and temperature $2.6^{+0.4}_{-0.3} \, \mathrm{keV}$ with an unabsorbed flux of $6.8 \times 10^{-6} \, \mathrm{photons} \, \mathrm{cm}^{-2} \, \mathrm{s}^{-1} \, \mathrm{deg}^{-2}$ at 10 keV. The best fit parameters for the exponentially cutoff power law model in this extended fit were $\Gamma = 0.52 \pm 0.25$ and energy cutoff $E_c = 39.4^{+11.2}_{-7.2} \, \mathrm{keV}$.

4. SUMMARY AND DISCUSSION

We have measured the spectrum of the Galactic X-ray/ γ -ray background near the Scutum arm region. In addition to the extrapolated high energy continuum (due to the interaction of cosmic rays with the interstellar medium) and the positron annihilation components, we have measured a variable hard X-ray/soft γ -ray component dominating the 10-200 keV

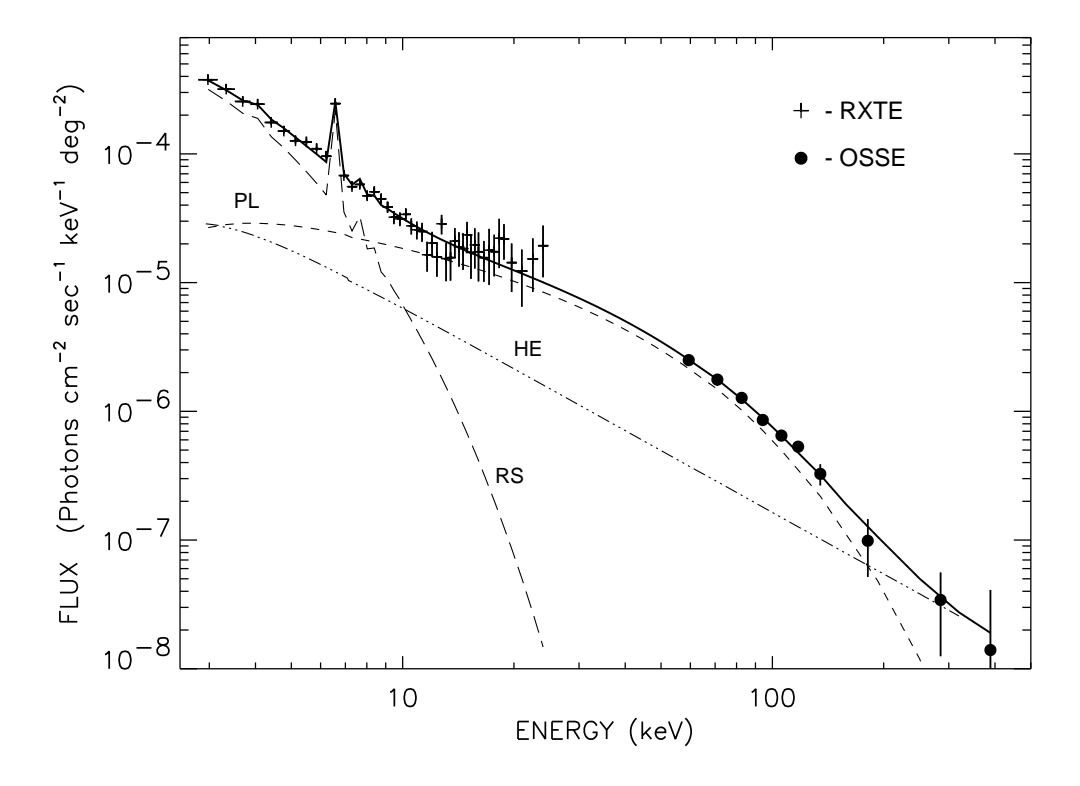


Fig. 2.— Unfolded RXTE/OSSE spectrum and the best fit models in the 3-400 keV band. OSSE spectrum from weeks 3 and 4 of the observation is used. The positron annihilation line and 3-photon positronium continuum components are subtracted from the OSSE data. The combined spectrum (top curve) is constructed by 3 components: a thermal Raymond-Smith plasma model (RS); an exponential cutoff power law model (PL); and a high energy continuum (HE) extrapolated to lower energies. Interstellar absorption is included as part of the model. See §3.2.2 for details.

band. The shape of this component at its minimum observed intensity is best modeled by an exponentially cut off power law of photon index of ~ 0.6 and energy cut off of ~ 41 keV. We estimate that at 60 and 100 keV, known bright discrete sources in the field of view of OSSE contribute about 46% and 20% to the total (minimum) measured flux, respectively.

The nature of the unresolved emission still remains to be determined. One interpretation is that the emission is due to a combination of unknown discrete sources. In the course of PCA scans, we detected several low luminosity discrete sources of the order of a few mCrabs for which we do not have a positive identification with previously known sources. We were not able to determine the spectral shape of these sources above ~ 20 keV because of the short exposures. The integrated 2-20 keV flux from these weak sources is a substantial fraction of the total of the previously identified sources listed in Table 1 if GRS1915+105 is excluded. It is then plausible that these weaker sources also make a significant contribution

to the flux detected with OSSE, and in this case a significant fraction of the 40-100 keV flux observed with OSSE would be due to discrete sources whose 2-10 keV flux is brighter than ~ 1 mCrab. The estimated 40-100 keV spectrum of the bright sources listed in Table 1 is softer than the total OSSE spectrum measured during the second viewing period (see §3.1). The spectrum of the remaining contributors would therefore have to be harder than that of the known sources reported in Table 1. While the spectrum during the second viewing period can be well fit with the standard pulsar model, the best-fit parameters are unusual. The HR of the model is higher than that of any pulsar in the review of White, Swank, & Holt (1983), higher than ever seen during the outburst of EXO 2030+375 (Reynolds, Parmar & White 1993), and higher than that of any of the pulsars in Table 1. While the HR of EXO 2030+375 decreased as its luminosity decreased, there is no clear dependence of the HR on luminosity for the pulsars reviewed by White, Swank, & Holt (1983). If the observed spectrum is dominated by unresolved pulsars, they must have much harder spectra than typically seen for X-ray pulsars. The spectra out to at least 40 keV is similar to that of the low state of black hole candidates (BHC) (e.g. Tanaka and Lewin 1995) since the unresolved spectrum can also be characterized with a broken power law model of photon indices of 1.4 and 3.3 and a break energy at 75.2 keV. Higher quality data are needed to determine if the form of the spectral break is similar to that of BHC.

An alternative interpretation for the origin of the unresolved emission is that it is truly of diffuse origin and is produced by mechanism(s) such as nonthermal electron bremsstrahlung or inverse Compton (IC) scattering of interstellar radiation off of cosmic-ray electrons (e.g. Skibo & Ramaty 1993). It is expected that the scale height of the emission due to IC scattering be broad because of the large scale height of the interstellar radiation field (optical, infrared, and the Cosmic microwave background). Indeed, the emission has been measured to be broad with RXTE (Valinia & Marshall 1998) and COMPTEL/CGRO (Strong et al. 1996b). Therefore, in the diffuse origin scenario, the hard spectral shape and the apparent broad extent of the emission would suggest the possibility that the IC scattering contribution may dominate over nonthermal bremsstrahlung processes. Unlike the nonthermal bremsstrahlung scenario, the IC scattering scenario has the added advantage that the total power required is well within that provided by Galactic supernovae.

Our discovery of variability in the 40-100 keV flux from the Galactic Ridge near Scutum shows that a substantial part of this emission is due to discrete sources. Determining the exact contribution of discrete sources and diffuse mechanism(s) to the total Galactic plane emission requires instruments capable of sensitive imaging over the hard X-ray/soft γ -ray band. A sensitivity of at least $10^{-6}-10^{-7}$ photons cm⁻² s⁻¹ keV⁻¹ at 100 keV and spatial resolution of a few arc minutes are required.

We thank David Band, Mark Finger, William Heindl, James Kurfess, Ed Morgan, and Mike Muno for helpful discussions. We also thank Keith Jahoda for help with the scanning response matrix for RXTE.

REFERENCES

- Bertsch, D. L. et al. 1993, ApJ, 416, 587
- Bloemen, H., et al. 1997, in Proc 4th Compton Symp., ed. C. Dermer, M. Strickman, & J. Kurfess (New York:AIP), 410, 1074
- Boggs, S. E., Lin, R. P., Slassi-Sennou, S., Coburn, W., & Pelling, R. M. 1999, astro-ph/9908170
- Corbet, R. H. D., Marshall, F. E., Peele, A. G., Takeshima, T. 1999, ApJ, 517, 956
- Hayakawa, S., Matsumoto, T., Murakami, H., Uyama, K., Thomas, J. A., Yamagami, T. 1981, A&A, 100, 116
- Hunter, S. D., et al. 1997, ApJ, 481, 205
- Hunter, S., Kinzer, R., & Strong, A. 1997, in Proc. 4th Compton Symp., ed. C. Dermer, M. Strickman, & J. Kurfess (New York: AIP), 410, 192
- Jahoda, K., Swank, J. H., Giles, A. B., Stark, M. J., Strohmayer, T., Zhang, W., & Morgan, E. H. 1996, Proc. SPIE, 2808, 59
- Johnson, W. N., et al. 1993, ApJS, 86, 693
- Kaneda, H. 1997, Ph.D. Dissertation, University of Tokyo
- Kinzer, R. L., Purcell, W. R., & Kurfess, J. D. 1999, ApJ, 515, 215
- Kniffen, D. A. & Fitchell, C. E., 1981, ApJ 250 389
- Koyama, K, Kawada, M., Takeuchi, Y., Tawara, Y., Ushimaru, N., Dotani, T., & Takizawa, M. 1990, ApJ, 356, L47
- Ore, A., & Powell, J. 1949, Phys. Rev., 75, 1696
- Reynolds, A. P., Parmar, A. N., & White, N. E., 1993, ApJ, 414, 302
- Pohl, M., 1998, A&A, 339, 587
- Purcell, W. R. et al. 1996, A&AS, 120, 389
- Sacher, W. & Schönfelder, V., 1984, ApJ 279 817
- Skibo, J. G., 1993, Ph.D. Dissertation, University of Maryland

Skibo, J. G. & Ramaty, R. 1993, A&AS, 97, 145

Skibo, J. G. et al. 1997, ApJ, 483, L95

Strong, A. W., et al. 1996a, ApJS, 120, 381

Strong, A. W., et al. 1996b, A&AS, 120, 381

Sunyaev, R. A., & Titarchuk, L. G., 1980, A&A, 86, 121

Tanaka, Y., & Lewin, W. H. G. 1995, in X-ray Binaries, ed. W. H. G. Lewin, J. van Paradijs, & E. P. J. van den Heuvel (Cambridge: Cambridge Univ. Press), 126

Valinia, A. & Marshall, F. E. 1998, ApJ, 505, 134

Van Paradijs, J. 1995, in X-ray Binaries, eds. W. H. G. Lewin, J. Van Paradijs & E. P. J. Van den Heuvel (Cambridge University Press), 536

White, N. E., Swank, J. H, Holt, S. S., 1983, ApJ, 270, 711

Yamasaki N. Y. et al. 1997, ApJ, 481, 821

Zhang, S. N. et al. 1996, A&AS, 120, 227

This preprint was prepared with the AAS LATEX macros v4.0.

Table 1. Bright Discrete Sources Within OSSE Field of View

Name	Flux (2-10 keV) ^a mCrab		OSSE ^b Response(%)	Flux at $60 \text{ keV}^{\text{c}}$ $10^{-5} \text{photons cm}^{-2} \text{s}^{-1}$		Flux at $100 \text{ keV}^{\text{d}}$ $10^{-6} \text{photons cm}^{-2} \text{s}^{-1}$	
	$W1-2^{e}$	W3-4 ^f	- , ,	W1-2e	$W3-4^{f,J}$	w1-2 ^e ,	i W3-4 ^{f,j}
A1845-024	9.1	3.9	69	0.7 (4%)	0.3~(3%)	1.5 (4%)	0.6~(2%)
XTE J1858+034	18.5	15.9	66	1.2~(6%)	1.1 (10%)	1.2 (3%)	1.1 (3%)
GS $1843+009$	12.3	6.4	54	5.1~(27%)	2.7~(24%)	6.7~(16%)	3.5~(11%)
$XTE\ J1855-026$	8.1	5.3	36	1.6~(9%)	1.0~(9%)	1.9~(5%)	1.2~(4%)
SS433	10.3	5.5	17	$0.1 \ (< 1\%)$	$0.06 \ (< 1\%)$	$0.07 \ (< 1\%)$	$0.04 \ (< 1\%)$
GRS1915 + 105	620	521	< 1	$\sim 0(0\%)$	$\sim 0(0\%)$	$\sim 0(0\%)$	$\sim 0(0\%)$
Total				8.7 (46%)	5.2 (46%)	11.4 (28%)	6.4 (20%)
Residual Flux ^k				10.1	5.8	29.4	26.3

^a Source flux from RXTE All Sky Monitor (ASM). Estimated RMS errors are typically 5%-20%.

^b OSSE's response at the position of the source.

^c Estimated source flux through OSSE's collimator (and the \sim % contribution of the sources to the total OSSE flux in each observation at 60 keV). This number has been determined by multiplying OSSE's response at the position of the source by the estimated flux of the source as described in the text.

^d Same as (c) except at 100 keV.

^e Averaged over weeks 1 and 2 of the observation.

^f Averaged over weeks 3 and 4 of the observation.

 $^{^{\}rm g}$ Total flux through OSSE's collimator averaged over weeks 1 and 2 was $1.88\times10^{-4}\,\rm photons\,cm^{-2}\,s^{-1}$ at 60 keV.

 $^{^{\}rm h}$ Total flux through OSSE's collimator averaged over weeks 3 and 4 was $1.10\times10^{-4}\,\rm photons\,cm^{-2}\,s^{-1}$ at 60 keV.

 $^{^{\}rm i}$ Total flux through OSSE's collimator averaged over weeks 1 and 2 was $4.08\times10^{-5}\,\rm photons\,cm^{-2}\,s^{-1}$ at 100 keV.

 $^{^{\}rm j}$ Total flux through OSSE's collimator averaged over weeks 3 and 4 was $3.27\times10^{-5}\,\rm photons\,cm^{-2}\,s^{-1}$ at 100 keV.

^kTotal measured OSSE flux minus the estimated contribution of discrete sources.